

Exploring PtSO₄ and PdSO₄ phases: an evolutionary algorithm based investigation

Hom Sharma,^a Vinit Sharma,^b and Tran Doan Huan^{*,b}

Metal sulfate formation is one of the major challenges to the emissions aftertreatment catalysts. Unlike the incredibly sulfation prone nature of Pd to form PdSO₄, no experimental evidence exists for the PtSO₄ formation. Given the mystery of nonexistence of the PtSO₄, we explore the PtSO₄ using a combined approach of evolutionary algorithm based search technique and quantum mechanical computations. Experimentally known PdSO₄ is considered for the comparison and validation of our results. We predict many possible low-energy phases of the PtSO₄ and PdSO₄ at 0K, which are further investigated under wide range of temperature-pressure conditions. An entirely new low-energy (tetragonal $P4_2/m$) structure of the PtSO₄ and PdSO₄ is predicted, which appears to be the most stable phase of the PtSO₄ and a competing phase of the experimentally known monoclinic $C2/c$ phase of PdSO₄. Phase stability at finite temperature is further examined and verified by free energy calculations of sulfates towards their possible decomposition products. Finally, temperature-pressure phase diagrams are computationally established for both PtSO₄ and PdSO₄.

1 Introduction

Sulfation (i.e. metal sulfate formation) of noble metal based catalysts has been a serious problem to automotive emissions aftertreatment systems.^{1–6} It is well established that Pd is extremely susceptible towards sulfation (i.e., the PdSO₄ formation) in the highly oxidizing and sulfating environment typically experienced by the aftertreatment catalysts. Unlike the easily formed sulfate PdSO₄ under catalytically relevant conditions, no experimental evidence is available for the existence of PtSO₄ under any circumstances.⁷ Despite being a member of the same group of the Periodic Table, an intriguing fact of non-existence of PtSO₄ remains as a puzzle and an unexplored territory. A question arises why PtSO₄ does not exist and what makes PtSO₄ different from PdSO₄? Answers to these questions may reveal the underlying mystery behind sulfation resistant phenomena of Pt and, in turn, provide some guidance for future design of sulfur resistant catalysts materials.

An experimental investigation based reaction pathway analysis suggested that the PdSO₄ formation is primarily due to the interaction between SO₃ and metal oxide (i.e., PdO) in the catalytically relevant temperature and pressure conditions⁸. Under similar experimental conditions, no PtSO₄ formation has been observed.^{9,10} In a recent study based on the first principle computations, Derzsi *et al.*⁷ suggested that the structure of PtSO₄ should be similar to that of PdSO₄ while assuming a similar nature of metal oxides (i.e. PdO and PtO) of Pd and Pt. Our recent work on Pt and Pd surfaces utilizing the first-principles thermodynamics suggested that the

PdSO₄ formation is indeed favored even at lower temperature pressure conditions; however, the PtSO₄ formation may be favorable only at elevated pressure conditions.¹¹ This outcome points out a direction for further investigations of the Pt and Pd sulfates under a wide range of temperature and pressure regimes, for which comprehensive information on the possible structural phases is required. Furthermore, PdSO₄ is stable towards decomposition to metal oxide (PdO) and sulfur oxides (SO₂/SO₃) below $\sim 650^\circ\text{C}$ ¹² which suggests that once the stable sulfate is formed, it is difficult to desulfate the catalysts. Unfortunately, such information is missing for PtSO₄ and needs an attention.

Our work is premised on the aforementioned mystery of contrasting behavior of Pt and Pd metals towards sulfation. We extensively explore the possible low-energy structures of the yet-to-be synthesized PtSO₄ and the known PdSO₄ using evolutionary algorithm-based method Universal Structure Predictor: Evolutionary Xtalloraphy (USPEX).^{13,14} Stability of the predicted low-energy structures are assessed by the evaluation of Gibbs free energy over a wide temperature-pressure range, fully considering the vibrational contributions calculated within the harmonic approximation. Furthermore, we investigate the stability of the predicted structures towards decomposition to their possible products. In this work, most notably we predict a tetragonal $P4_2/m$ structure (no. 84) to be the lowest in energy for both PtSO₄ and PdSO₄. Interestingly, we find that the experimentally-known monoclinic $C2/c$ phase (no. 15) of PdSO₄ is energetically competing with the newly identified $P4_2/m$ phase. Moreover, we construct phase diagrams of the PtSO₄ and PdSO₄ over a range of temperature and pressure which shows the stability of various sulfate phases.

^a Department of Chemical and Biomolecular Engineering, University of Connecticut, Storrs, CT 06269 USA.

^b Material Science and Engineering, University of Connecticut, Storrs, CT 06269 USA

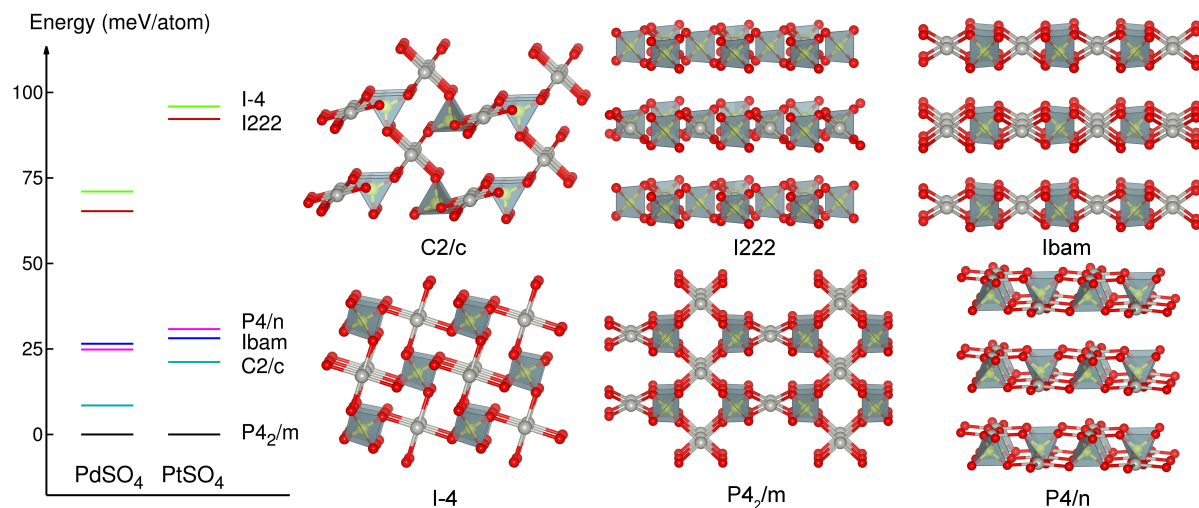


Fig. 1 Relative energetics (enthalpies) and structures of the selected low energy phases of PdSO_4 and PtSO_4 predicted using USPEX method. Pt (or Pd), S, and O atoms are represented by silver, yellow, and red colors, respectively.

2 Methods

Possible stable structures of PdSO_4 and PtSO_4 are searched using an evolutionary search technique embodied in USPEX code.^{13,14} The code/method, predicts the crystal packing from only a knowledge of chemical species, compositions, or the molecular geometries, has met tremendous success in correctly identifying and predicting the crystal structures of various classes of systems (bulk crystals,^{15,16} nanoclusters,¹⁷ 2D crystals,¹⁸ surfaces,¹⁹ and new polymers^{20,21}). In this work, we explored the structural space of PtSO_4 and PdSO_4 , with a fixed stoichiometric composition, allowing up to four formula units per unit cell. The energy ordering, lattice parameters, and the electronic structures of the identified phases are determined within the framework of density functional theory (DFT) using the all electron projector augmented wave method^{22,23} as implemented in Vienna *Ab initio* Simulation Package (VASP) code.^{24,25} Our DFT calculations are performed within the generalized gradient approximation using the Perdew-Burke-Ernzerhof (PBE) exchange-correlation (XC) functional.^{26,27} It is worth mentioning that the energy ordering is invariant with respect to the choice of the XC functional. All the plane waves with kinetic energy up to 500 eV was used in our basis set. To sample the Brillouin zone, we employed Monkhorst-Pack \mathbf{k} -point mesh producing the convergence within 1 meV per formula unit. The atomic positions are optimized by relaxing all the atoms until the Hellman-Feynman forces become less than 0.01 eV/Å. The density of states (DOS) is calculated by the linear tetrahedron method with Blöchl corrections.

Dynamical stability of all the selected structural candidates

is confirmed by the phonon frequency spectra calculated using the finite-displacement approach as implemented in the PHONOPY code.^{29,30} To establish the stability of the predicted phases at finite temperature and pressure, relevant thermodynamic properties were evaluated from the computed phonon band spectra. FullProf suite³¹ was used to simulate the X-ray diffraction patterns.

3 Results and discussion

3.1 Low-energy structures of PdSO_4 and PtSO_4

The evolutionary algorithm based search for ground-state phases of PdSO_4 and PtSO_4 resulted in a large number of possible low-energy structures. Total six such low-energy structures (in right panel) for both cases (i.e. PtSO_4 and PdSO_4) and their relative energy (in left panel) are shown in the Figure 1. The $P4_2/m$ phase is predicted to be the most stable phase of both PdSO_4 and PtSO_4 . The experimentally known $C2/c$ structure³² of PdSO_4 is energetically very similar (within the computational error limit) as a competing phase. However, the $P4_2/m$ phase of PtSO_4 is significantly lower in energy than the second most stable phase $C2/c$. More specifically, the energy difference between the $C2/c$ and the $P4_2/m$ structures is ~ 8 meV/atom and ~ 21 meV/atom for PdSO_4 and PtSO_4 , respectively. Orthorhombic $Ib\bar{a}m$ (no. 72), tetragonal $P4/n$ (no. 85) phases of both are relatively similar in energetics, notably the orthorhombic $I222$ (no. 23), and tetragonal $I\bar{4}$ (no. 82) structures of PtSO_4 are less stable compared to the same structures of PdSO_4 . Structural information (lattice parameters, atomic coordinates etc.) for all the phases of PdSO_4 and PtSO_4 shown

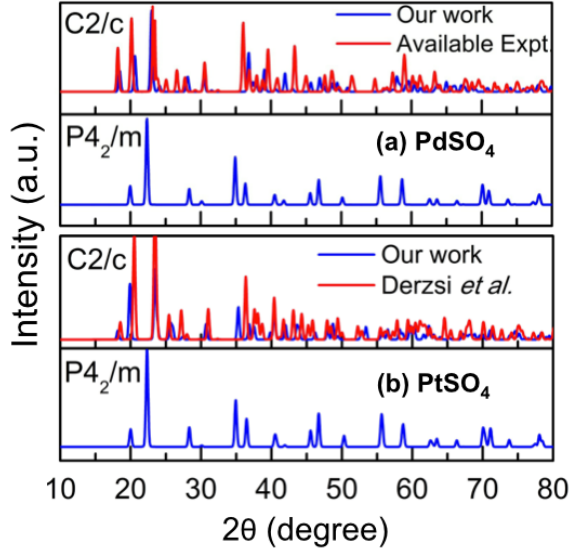


Fig. 2 Simulated XRD patterns two low-energy structures predicted for (a) PdSO_4 and (b) PtSO_4 at ambient pressure. For PdSO_4 , the XRD pattern of the monoclinic $C2/c$ is shown using the available experimental data/parameters.²⁸ For PtSO_4 , the simulated XRD pattern of the predicted $C2/c$ structure is compared to that of the $C2/c$ phase suggested by Derzsi *et al.*⁷

in Figure 1 is given in the Supporting Information (see Table S1).

The predicted low-energy structures of both sulfates are morphologically similar. Each structure consists of tetrahedral SO_4 groups, where O atoms are associated to four different SO_4 tetrahedra coordinating the Pd atoms in a plane. The local chemistry at the anionic site, the topology and the connectivity of the crystal networks are also qualitatively similar in both sulfates. In general, these six structures can be classified into two groups. The first structure type, with a non-layered 3-D network, contains oxygen atoms from the SO_4 unit which act as a bridge (for example: $P4_2/m$, $C2/c$, and $I4$ phases) linking metal atoms. The second structure type involves some two-dimensional motifs with isolated layers of Pd/Pt and SO_4 tetrahedra (for example: $Ibam$, $P4/n$, and $I222$ phases).

We further analyzed the selected low-energy structures by simulating the X-ray diffraction (XRD) patterns. In Figure 2 (top panels), we show the XRD simulations of $C2/c$ and $P4_2/m$ phases of PdSO_4 along with the available experimental XRD data of $C2/c$ phase.²⁸ In bottom panels (Figure 2), we show the XRD simulations of our predicted $C2/c$ and $P4_2/m$ phases along with the suggested $C2/c$ phase of PtSO_4 by Derzsi *et al.*⁷ Overall, the simulated peaks in XRD plot are in good agreement with the available experimental data.²⁸ The additional XRD simulations (of the other predicted phases) are given in the Supporting Information S2.

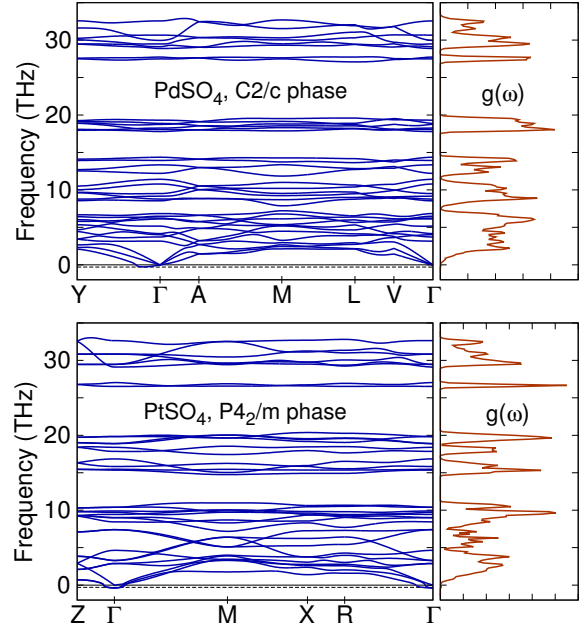


Fig. 3 (Color online) Phonon band structures (left panels) and density of phonon states $g(\omega)$ (right panels, given in arbitrary units), of the $P4_2/m$ phase of PtSO_4 (top panel) and the $C2/c$ phase of PdSO_4 (bottom panel) at $P = 0$ GPa. For convenience, bands with imaginary frequencies are shown as those with *negative* frequencies. Within the error bar (indicated by the dotted lines) of ~ 0.3 THz due to the translational symmetry breaking while calculating the XC energies by VASP, no imaginary phonon modes appear throughout the Brillouin zones of the two structures examined.

3.2 Dynamical and thermodynamic stabilities

Next, we examined the dynamical stability of all predicted low-energy structures of PtSO_4 and PdSO_4 using the calculated phonon band structures. No imaginary modes exist throughout the Brillouin zones of these structures, demonstrating that they are dynamically stable. For illustration, we show in Fig. 3 the phonon spectra and the phonon density of states $g(\omega)$ we calculated for the lowest-energy structures of each compound, i.e., the $P4_2/m$ structure of PtSO_4 and the $C2/c$ structure of PdSO_4 . Similar information for all other predicted structures can be found in the Supporting Information S3.

The phonon spectra of these structures, calculated at 0K, allow estimating the vibrational contribution $F_{\text{vib}}(T)$ to the Gibbs free energy $G(P, V, T) = E_{\text{DFT}} + F_{\text{vib}}(T) + PV$ within the harmonic approximation via

$$F_{\text{vib}}(T) = rk_{\text{B}}T \int_0^\infty d\omega g(\omega) \ln \left[2 \sinh \left(\frac{\hbar\omega}{2k_{\text{B}}T} \right) \right], \quad (1)$$

where, r is number of degrees of freedom in the unit cell, k_{B} is the Boltzmann's constant, \hbar is the reduced Planck's constant, and $g(\omega)$ is the normalized phonon density of state at

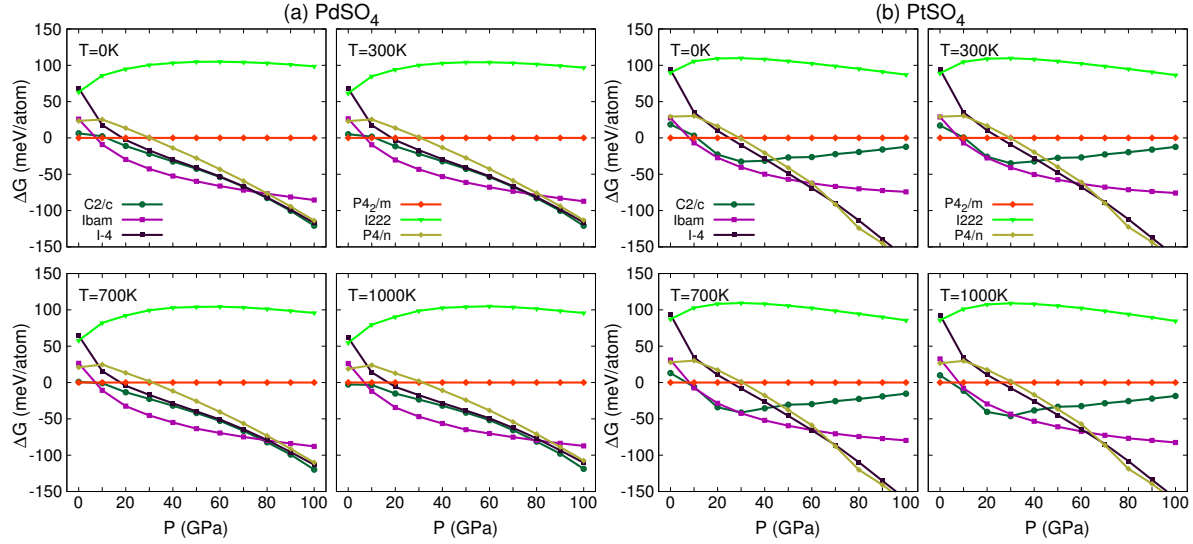


Fig. 4 Gibbs free energies with entropic contributions, G calculated at $T = 0\text{K}$, $T = 300\text{K}$, $T = 700\text{K}$, and $T = 1000\text{K}$ for the identified low-energy structures of PdSO_4 (panel a) and PtSO_4 (panel b) are shown as functions of pressure P . Data is given by symbols while curves are guides to the eye.

frequency ω . For hard crystalline materials, the method provides a good way to access their thermodynamic stability and typically yields an excellent agreement with experimental data (see, for example, Ref.³³).

Our calculations for $G(P, V, T)$ are summarized in Figure 4. Results suggest that the $P4_2/m$ phase of PtSO_4 is the thermodynamically stable at low pressures and over the temperature range considered. In the case of PdSO_4 , the $C2/c$ structure (which is experimentally established³²) is very slightly less stable than the $P4_2/m$ structure by ~ 2 meV at low pressures and temperatures. According to our calculations, the $C2/c$ phase becomes thermodynamically stable at above 700K. We note that the energy difference between these structures are comparable within the accuracy of DFT and both structures are energetically competing phases of PdSO_4 . The formation of the $C2/c$ phase, which is observed even at low temperatures conditions, may be driven by kinetics, which is well-known under the empirical Ostwald's steps rules in crystal nucleation.

Our calculations for $G(P, V, T)$ are summarized in Figure 4. Results suggest that the $P4_2/m$ phase of PtSO_4 is the thermodynamically stable at low pressures and over the temperature range considered. In the case of PdSO_4 , the $C2/c$ structure (which is experimentally established³²) is very slightly less stable than the $P4_2/m$ structure by ~ 2 meV at low pressures and temperatures. According to our calculations, the $C2/c$ phase becomes thermodynamically stable at above 700K. We note that the energy difference between these structures are comparable within the accuracy of DFT and both structures are energetically competing phases of PdSO_4 . The formation of the $C2/c$ phase, which is observed even at low temperatures

conditions, may be driven by kinetics, which is well-known under the empirical Ostwald's steps rules in crystal nucleation.

Both PdSO_4 and PtSO_4 undergo several structural phase transitions at higher pressures. For PdSO_4 , the orthorhombic $Ibam$ phase is stable within a wide range of pressure from ~ 10 to ~ 80 GPa before transforming to the tetragonal $I\bar{4}$ phase. The phase boundaries depend weakly on temperature. While the $Ibam$ phase is clearly thermodynamically most stable between 10 and 80 GPa, the monoclinic $C2/c$ and the tetragonal $P4/n$ are energetically competing with the $I\bar{4}$ phase above 80 GPa. The energy differences between these phases are small compared to the thermal energy $k_B T$, especially at the high limit of T . Unlike the PdSO_4 , the $C2/c$ phase of PtSO_4 is more stable only at high temperature ($> 700\text{K}$) and slightly elevated pressure (> 10 GPa) conditions while the $Ibam$ phase is stable at lower temperatures ($< 700\text{K}$) and elevated pressure (10–60 GPa) conditions. The transition between the $Ibam$ phase to either the $I\bar{4}$ or the $C2/c$ phase occurs at roughly around 60 GPa. For both PdSO_4 and PtSO_4 , the $I222$ phase is unstable over the whole range of pressure examined.

Utilizing the information about the phase stability from Figure 4, we constructed the phase diagrams of both sulfates from the calculated free energy $G(P, V, T)$ as shown in Figure 5. The phase diagrams display a map of the stable phases over the range of T - P conditions. Most importantly, we observed that the tetragonal $P4_2/m$ is a sole candidate for atmospheric pressure and relevant temperature pressure conditions. However, $P4_2/m$ and $C2/c$ phases are the important phases in the similar conditions. Furthermore, the $Ibam$ phase dominates the

10–60 GPa region for both cases, which could be an interest of exploration for the high pressure applications.

While experimental studies suggest that PdSO_4 decomposes above $\sim 900\text{K}$ ⁸, estimation of free energy of reaction (ΔG) over a range of temperature allows us to evaluate the thermodynamic stability (reaction feasibility) of the compound towards decomposition to its products. The feasibility of a reaction depends on the sign of ΔG , which is equal to $\Delta H - T\Delta S$, where ΔH is the change in enthalpy and ΔS is the change in entropy. The ΔG of the reaction can be expressed as:

$$\Delta G = \sum_{i=1}^n G_{\text{products}} - \sum_{i=1}^n G_{\text{reactants}}. \quad (2)$$

In this work, we considered the decomposition reaction of Pd(or Pt) SO_4 towards their respective most stable metal oxides and sulfur oxide species [i.e. $\text{Pd(or Pt)SO}_4 \rightarrow \text{Pd(or Pt)O} + \text{SO}_3$]. For example, the computed ΔG values at 300K were ~ -60 kJ/mol and ~ -40 kJ/mol for PdSO_4 and PtSO_4 , respectively. Furthermore, we evaluated the free energy of the decomposition of the sulfates to their respective elemental species (i.e. $\text{Pd (or Pt) SO}_4 \rightarrow \text{Pd(or Pt)} + \text{S} + 2\text{O}_2$). The computed ΔG values were in the range of ~ -500 kJ/mol at 300K. Results suggest that PdSO_4 is stable towards decomposition to PdO and SO_3 below 775K whereas PtSO_4 stability towards PtO and SO_3 remains below 650K. Similarly, PdSO_4 is stable towards the decomposition to the elemental components below 870K whereas PtSO_4 is stable below 800K. In general, our calculations show that PdSO_4 is more stable than PtSO_4 towards decomposition for a particular temperature. Our results are in good agreement, given the computational error range in energetics, with the available experimental results of PdSO_4 decomposition stability. Furthermore, synthesis of PtSO_4 seems feasible in the future given the kinetic barriers are easy enough to cross. The free energy (ΔG) versus temperature (T) plot is given in Supporting Information S4.

To further confirm whether these sulfates are stable or not with respect to the pool of all possible product species, a linear programming (LP) algorithm^{34,35} has been employed. Here, a Pd(or Pt) SO_4 compound is considered to be stable when ΔE (the DFT energy relative to the best outcome from the LP) is negative. The energy difference, ΔE , can thus be written as

$$\Delta E = \text{Pd(or Pt)SO}_4 - \min \sum_{i=1}^n c_i P_i, \quad (3)$$

where P_i represents all the possible stable chemical species (i.e. for PdSO_4 : Pd, PdO, SO_3 , SO_2 , SO, S, and O_2 ; for PtSO_4 : Pt, PtO_2 , PtO, SO_3 , SO_2 , SO, S, and O_2). For example, the equation for PdSO_4 becomes $\Delta E = \text{PdSO}_4 - \min(c_1 \text{Pd}_{a_1} + c_2 \text{Pd}_{a_2} \text{O}_{o_2} + c_3 \text{S}_{b_3} \text{O}_{3o_3} + c_4 \text{S}_{b_4} \text{O}_{2o_4} + c_5 \text{S}_{b_5} \text{O}_{o_5} + c_6 \text{S}_{b_6} +$

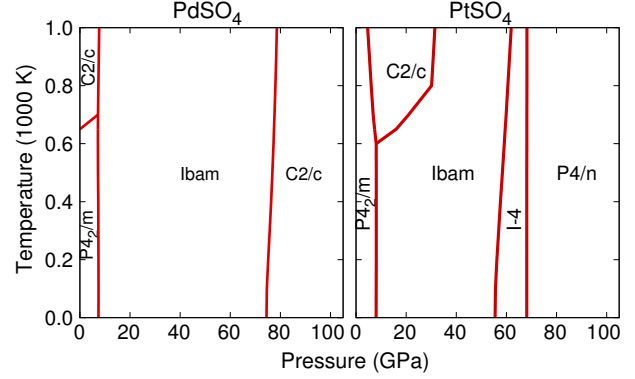


Fig. 5 Computed phase diagrams of PdSO_4 (left panel) and PtSO_4 (right panel). Thermodynamically stable phases are shown as indicated by their space group symbols.

$c_7 \text{O}_{2o_7}$). Then, the LP problem is solved with the constraints

$$\sum_i a_i c_i = 1, \sum_i b_i c_i = 1, \text{ and } \sum_i o_i c_i = 4, \quad (4)$$

where a_i , b_i , and o_i represent Pt(or Pd), S, and O content of a species, respectively. Above constraints ensure the correct stoichiometry of Pd(or Pt) SO_4 and with

$$c_i \geq 1, \quad (5)$$

which warrants that only the references containing Pt(or Pd), S, or O are taken into account. With all DFT computed energies of the species, we obtained all the optimized c_i and ΔE for each case. Consistent with our free energy of reaction analysis, negative ΔE values (i.e. -0.87 eV and -0.70 eV for PdSO_4 and PtSO_4 , respectively) were obtained, which confirmed the stability of the sulfates. Interestingly, we obtained mono-metallic oxides (PdO and PtO in the case of PdSO_4 and PtSO_4 , respectively) and SO_3 as possible decomposition products, consistent with our reaction free energy analysis, and unity (as expected) for all c_i values.

3.3 Electronic structures

We investigated the electronic structures of all low-energy phases of PdSO_4 and PtSO_4 by computing the total density of states. Overall, our results show no significantly different behavior between the phases of both sulfates. For better understanding the DOS can be divided into three main groups. First, the lower valence bands (between -2 eV and -4 eV) originate due to mixing of the valence d and p states of Pd(or Pt) and the O atoms. In this region, Pd(or Pt) (d) bands are found to be highly resonant with the O (p) bands. We also noticed that some pronounced mixing between the segments of O (p) bands lying above and below the valence Pd(or Pt) (d)

bands. Second, in the vicinity of the Fermi level the valence-band maximum are dominated by Pd(or Pt) (*d*) states. Third, the bottom of the conduction band consists 3*p* states of S and O (2*p*) states. Further detail can be found in the Supporting Information S5.

4 Conclusions

In summary, we explored the mystery of PtSO₄ non-existence using evolutionary algorithms based method and the first principles computations. We considered the known PdSO₄ for the comparison and validation of our approach. Many low-energy structures are predicted and analyzed for the stability in a wide range of temperature and pressure conditions. We identify a new stable tetragonal *P4₂/m* structure for both metal sulfates. We predicted that the *P4₂/m* phase is the most stable phase of PtSO₄ and a competing structure with monoclinic *C2/c* phase of PdSO₄. Based on the computed Gibbs free energies, we constructed phase diagrams which provide reliable information about the phases stability, phase transition, and their boundaries in a wide range of temperature and pressure conditions. Phase diagrams confirmed the existence of experimentally observed monoclinic *C2/c* phase of PdSO₄ at the ambient conditions; however, this phase may not be seen in the case of PtSO₄ in similar conditions. Nonetheless, *Ibam* phase remains one of the promising stable phase for both cases at high pressure conditions. Both sulfates were stable towards decomposition to their possible products well above the room temperature, which also suggests the possibility of PtSO₄ synthesis in the future. In general, we provide a detailed information on the phases and their stability of PdSO₄ and PtSO₄ which can be helpful to understand the sulfating nature of Pd and design/scan promising new sulfur resistant materials.

Acknowledgement

HNS acknowledges the United States Environmental Protection Agency (EPA) STAR graduate fellowship, fellowship number FP917501, for funding support. Its contents are solely the responsibility of the fellow and do not necessarily represent the official views of the EPA. Finally, Authors acknowledge Materials Design[®] for MedeA[®] software and thank School of Engineering, UCONN for Hornet supercomputer access.

Supplementary Information

Electronic Supplementary Information (ESI) available: Structural information of PtSO₄ and PdSO₄ are shown in S1, XRD patterns of the predicted structures are shown in S2, the phonon density of states are shown in S3, free energy diagram is given in S4, and electronic density of states are shown in S5 of the Supplementary Information.

*Corresponding author: huan.tran@uconn.edu

References

- 1 H. N. Sharma, S. L. Suib and A. B. Mhadeshwar, in *Interactions of Sulfur Oxides With Diesel Oxidation Catalysts (DOCs)*, American Chemical Society, Washington, DC, 2013, vol. 1132, pp. 117–155.
- 2 A. Russell and W. S. Epling, *Catal. Rev.*, 2011, **53**, 337–423.
- 3 H. C. Yao, H. K. Stepien and H. S. Gandhi, *J. Catal.*, 1981, **67**, 231–236.
- 4 C. P. Hubbard, K. Otto, H. S. Gandhi and K. Y. S. Ng, *Catal. Lett.*, 1994, **30**, 41–51.
- 5 C. P. Hubbard, K. Otto, H. S. Gandhi and K. Y. S. Ng, *J. Catal.*, 1993, **144**, 484–494.
- 6 S. Koutsopoulos, S. B. Rasmussen, K. M. Eriksen and R. Fehrmann, *Appl. Catal. A: Gen.*, 2006, **306**, 142–148.
- 7 M. Derzsi, A. Hermann, R. Hoffmann and W. Grochala, *Eur. J. Inorg. Chem.*, 2013, **2013**, 5094–5102.
- 8 D. L. Mowery, M. S. Graboski, T. R. Ohno and R. L. McCormick, *Appl. Catal. B: Env.*, 1999, **21**, 157–169.
- 9 G. Corro, *React. Kinet. Catal. Lett.*, 2002, **75**, 89–106.
- 10 U. Köhler and H. W. Wassmuth, *Surf. Sci.*, 1983, **126**, 448–454.
- 11 H. Sharma, V. Sharma, A. Mhadeshwar and R. Ramprasad, Submitted to *J. Chem. Phys. Lett.*
- 12 A. K. Neyestanaki, F. Klingstedt, T. Salmi and D. Y. Murzin, *Fuel*, 2004, **83**, 395–408.
- 13 C. W. Glass, A. R. Oganov and N. Hansen, *Comput. Phys. Commun.*, 2006, **175**, 713–720.
- 14 A. R. Oganov and C. W. Glass, *J. Chem. Phys.*, 2006, **124**, 244704.
- 15 A. R. Oganov and C. W. Glass, *J. Chem. Phys.*, 2006, **124**, 244704.
- 16 A. R. Oganov, A. O. Lyakhov and M. Valle, *Acc. Chem. Res.*, 2011, **44**, 227–237.
- 17 X.-F. Zhou, X. Dong, A. R. Oganov, Q. Zhu, Y. Tian and H.-T. Wang, *Phys. Rev. Lett.*, 2014, **112**, 085502.
- 18 A. O. Lyakhov, A. R. Oganov, H. T. Stokes and Q. Zhu, *Comp. Phys. Comm.*, 2013, **184**, 1172–1182.
- 19 Q. Zhu, L. Li, A. R. Oganov and P. B. Allen, *Phys. Rev. B*, 2013, **87**, 195317.
- 20 V. Sharma, C. C. Wang, R. G. Lorenzini, R. Ma, Q. Zhu, D. W. Sinkovits, G. Pilania, A. R. Oganov, S. Kumar, G. A. Sotzing, S. A. Boggs and R. Ramprasad, *Nat. Comm.*, 2014, **5**, 4845.
- 21 Q. Zhu, V. Sharma, A. R. Oganov and R. Ramprasad, *J. Chem. Phys.*, 2014, **141**, 154102.
- 22 W. Kohn and L. J. Sham, *Phys. Rev.*, 1965, **140**, A1133–A1138.
- 23 P. Hohenberg and W. Kohn, *Phys. Rev.*, 1964, **136**, B864–B871.
- 24 G. Kresse and J. Furthmüller, *Phys. Rev. B*, 1996, **54**, 11169.
- 25 G. Kresse and J. Furthmüller, *Comput. Mater. Sci.*, 1996, **6**, 15–50.
- 26 J. P. Perdew, K. Burke and M. Ernzerhof, *Phys. Rev. Lett.*, 1996, **77**, 3865–3868.
- 27 P. E. Blöchl, *Phys. Rev. B*, 1994, **50**, 17953–17979.
- 28 D. L. Mowery and R. L. McCormick, *Appl. Catal. B: Env.*, 2001, **34**, 287–297.
- 29 A. Togo, F. Oba and I. Tanaka, *Phys. Rev. B*, 2008, **78**, 134106.
- 30 K. Parlinski, Z. Q. Li and Y. Kawazoe, *Phys. Rev. Lett.*, 1997, **78**, 4063–4066.
- 31 J. Rodríguez-Carvajal, *Physica B*, 1993, **192**, 55.
- 32 T. Dahmen, P. Rittner, S. Böger-Seidl and R. Gruehn, *J. Alloy Compd.*, 1994, **216**, 11–19.
- 33 T. D. Huan, V. Sharma, G. A. Rossetti, Jr. and R. Ramprasad, *Phys. Rev. B*, 2014, **90**, 064111.
- 34 I. E. Castelli, D. D. Landis, K. S. Thygesen, S. Dahl, I. Chorkendorff, T. F. Jaramillo and K. W. Jacobsen, *Energy Environ. Sci.*, 2012, **5**, 9034–9043.
- 35 V. Ozolins, E. H. Majzoub and C. Wolverton, *J. Am. Chem. Soc.*, 2009, **131**, 230–237.